Shapes of single bubbles in infinite stagnant liquids contaminated with surfactant

Aoyama, Shohei
Hayashi, Kosuke
Hosokawa, Shigeo
Tomiyama, Akio

(Citation)
Experimental Thermal and Fluid Science,96:460-469

(Issue Date)
2018-09

(Resource Type)
journal article

(Version)
Accepted Manuscript

(URL)
https://hdl.handle.net/20.500.14094/90004933

Shapes of single bubbles in infinite stagnant liquids contaminated with surfactant

Shohei Aoyama, Kosuke Hayashi, Shigeo Hosokawa, Akio Tomiyama *

Graduate School of Engineering, Kobe University, 1-1, Rokkodai, Nada, Kobe 657-8501, Japan

**Corresponding author: tomiyama@mech.kobe-u.ac.jp, Tel/Fax: +81-78-803-6131*

Keywords: Contaminated bubble, Aspect ratio, Surfactant, Correlation

H I G H L I G T S

· Effects of surfactant on bubble shape are experimentally investigated.

· Triton X-100, 1-octanol, SDS and 1-decanol are used for surfactant.

· A correlation of aspect ratio is proposed based on experimental data.

A B S T R A C T

Aspect ratios of ellipsoidal bubbles in clean and contaminated systems were measured to investigate the effects of surfactant on the bubble aspect ratio. The bubble diameter ranged from 0.80 to 5.8 mm. Air was used for the gas phase and the glycerol-water solutions were used for the liquid phase. The experimental ranges of the Morton number, M, the bubble Reynolds number, Re, the Eötvös number, Eo, the Weber number, We, and the Tadaki number, Ta, were as follows: $10^{-7} < M < 10^{-3}$, $3.6\times10^{-1} < Re < 1.7\times10^{2}$, $1.1\times10^{-1} < Eo < 5.9$, $5.0\times10^{-3} < We < 3.7$ and $5.3\times10^{-2} < Ta < 3.6$. Triton X-100 and 1-octanol were used for surfactant. The terminal velocities of bubbles were confirmed to be independent of the surfactant concentration, and therefore, the bubbles were fully-contaminated from the point of view of the terminal velocity. By making use of the aspect ratio data, the applicability of available aspect ratio correlations was examined and an empirical correlation was proposed. The applicability of the proposed correlation was also examined for sodium dodecyl sulphate (SDS) and 1-decanol. As a result, the following conclusions were obtained: (1) the aspect ratio database, which is of use for validating and developing shape correlations, was obtained, (2) the available aspect ratio correlations are not applicable to the present data for fully-contaminated ellipsoidal bubbles, (3) the aspect ratios are well correlated in terms of a combination of the Eötvös and bubble Reynolds numbers, which proves that all the relevant forces, i.e.

the viscous, inertial, buoyant and surface tension forces, should be taken into account to correlate bubble shapes, and (4) the empirical correlation of the aspect ratio developed by using the Triton X-100 and 1-octanol data also gives good evaluations for bubbles contaminated with SDS and 1-decanol in spite of largely different adsorption-desorption characteristics.

---

1. Introduction

Knowledge on the shapes of bubbles is of great importance in modelling forces acting on a bubble such as drag and lift forces and interfacial heat and mass transfer (Clift et al., 1978). The shape deformation of an ellipsoidal bubble has often been evaluated using the aspect ratio, E, the ratio of the bubble minor axis to the major axis, and available models of the forces and the interfacial heat and mass transfer express the effects of the shape deformation in terms of E (Lamb, 1932; Lochiel and Calderbank, 1964; Moore, 1965; Clift et al., 1978; Tomiyama et al., 2002a; Tomiyama et al., 2002b; Tomiyama et al., 2004; Rastello et al., 2011). Many studies on E of clean bubbles have been carried out and several correlations of E have been proposed (Tadaki and Maeda, 1961; Moore, 1965; Wellek et al., 1966; Vakhrushev and Efremov, 1970; Fan and Tsuchiya, 1990; Raymond and Rosant, 2000; Myint et al., 2007; Sugihara et al., 2007; Loth, 2008; Legendre et al., 2012; Liu et al., 2015; Aoyama et al., 2016). We (Aoyama et al., 2016) carried out experiments on the shapes of ellipsoidal bubbles in infinite stagnant clean liquids at intermediate Morton numbers, M, i.e. $10^{-6.6} \leq M \leq 10^{-3.9}$, and examined the applicability of available correlations of E (Tadaki and Maeda, 1961; Moore, 1965; Wellek et al., 1966; Fan and Tsuchiya, 1990; Myint et al., 2007; Sugihara et al., 2007; Legendre et al., 2012) to the data. Since they could not give good agreements with the data, we proposed a new correlation of E by taking into account all the forces acting on a bubble, i.e. the inertial, viscous, buoyant and surface tension forces, in terms of the two dimensionless numbers, the bubble Reynolds number, Re, and the Eötvös number, Eo. The proposed correlation gives good evaluations of E for a wide range of M.

The shape and motion of bubbles are known to be affected by the presence of surface-active agents (surfactant) (Fan and Tsuchiya, 1990; Bel Fdhila and Duineveld,

1996; Tomiyama et al., 1998; Fukuta et al., 2008; Takagi et al., 2009). The surfactant decreases the surface tension and a non-uniform distribution of the surface tension at bubble interface causes a force tangential to the interface, i.e. the Marangoni effect, which is the cause of the retardation of interface motion of a rising bubble and the decrease in bubble rise velocity (Levich, 1962). The surface tension reduction and the Marangoni effect may also affect E. Our knowledge on the surfactant effect on E is however still insufficient. A correlation of E for contaminated bubbles was proposed by Vakhrushev and Efremov (1970). They expressed E in terms of the Tadaki number. Fan and Tsuchiya (1990) modified the Vakhrushev-Efremov correlation to improve its accuracy. Loth (2008) collected available experimental data of E of contaminated bubbles and proposed an E correlation for the data. Although an E correlation proposed by Wellek et al. (1966) is for contaminated drops, it has often been used for both bubbles and drops. However the applicable ranges of these correlations are still unclear due to lack of experimental data.

Aspect ratios of single ellipsoidal bubbles in infinite stagnant liquids contaminated with surfactant were measured in this study. Triton X-100 and 1-octanol were used for surfactant. These surfactants have often been used in investigations of the surfactant effects on bubble dynamics (Takagi et al., 2009; Aoki et al., 2015). The former is non-ionic surfactant and forms micelles at concentrations larger than the critical micelle concentration (CMC). The latter is an alcohol, whereas it accumulates at the gas-liquid interface and behaves like surface-active agent. We focused only on the fully-contaminated condition, in which the terminal velocity of a bubble is independent of the surfactant concentration. Even though bubbles are fully-contaminated from the point of view of the terminal velocity, the surface tension decreases with increasing the surfactant concentration (up to CMC for Triton X-100). Therefore the increase in the surfactant concentration may affect E. Two concentrations were used for each surfactant to investigate this effect. The concentrations of Triton X-100 were less than CMC for this purpose. The applicability of the above-mentioned E correlations was examined by comparing with the data. Then an empirical correlation for contaminated bubbles was developed by taking into account all the forces acting on a bubble as has been carried out in Aoyama et al. (2016).

2. Experimental

Figure 1 shows the experimental setup, which consists of the tank made of transparent acrylic resin and the nozzle. The width, depth and height of the tank were 0.20, 0.20 and 0.63 m, respectively. Since the maximum bubble diameter in the present experiment was 5.80 mm, the tank size was large enough to make the wall effect on the motion and shape of a bubble negligible (Clift et al., 1978). Single bubbles were formed from the nozzle tip by injecting air from the syringe A. Small amount of the liquid was also supplied from the syringe L so as to make bubbles fully-contaminated during a long-term two-phase contact in the bubble formation process. The inner diameter of the nozzle was varied from 0.51 to 4.01 mm to form single bubbles of various sizes, i.e. the sphere-volume-equivalent bubble diameter, d, was ranged from 0.80 to 5.80 mm. Successive bubble images were taken by using a high-speed video camera (Integrated Design Tools, M5; frame rate: 100-170 frames/s; exposure time: 100 μs). The spatial resolution was varied from 1.15×10^{-2} to 1.26×10^{-2} mm/pixel, so that the number of pixels for d of the minimum bubble was 70. An image processing method (Aoyama et al., 2016) was used to measure d, E and the bubble velocities V_B, where E is defined by

$$E=\frac{d_V}{d_H} \tag{1}$$

where d_H and d_V are the bubble major and minor axes, respectively. The uncertainties in d, E and V_B estimated at 95% confidence were 1.7%, 2.7% and 0.91%, respectively.

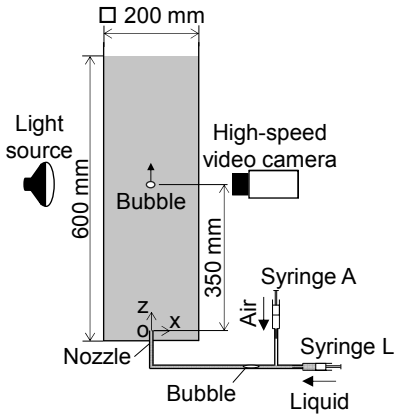

Fig. 1 Experimental setup

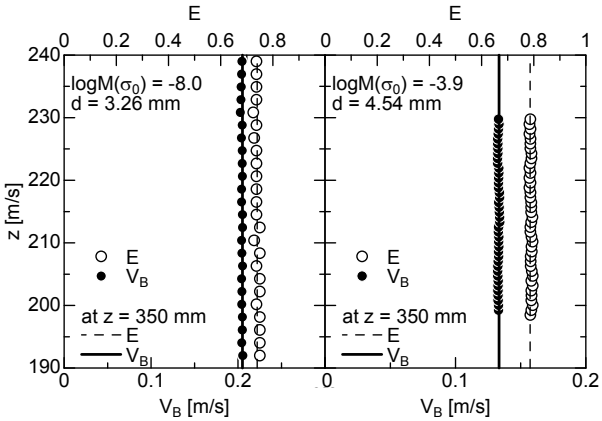

Fig. 2 Time evolution of E and V_B after bubble release (C_T = 0.10 mol/m^3)

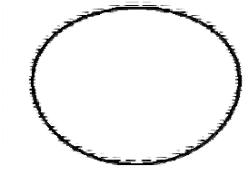

(a) log$M$(σ_0) = –8.0, d = 2.97 mm

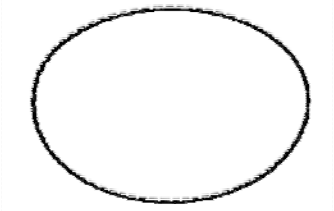

(b) log$M$(σ_0) = –6.7, d = 3.74 mm

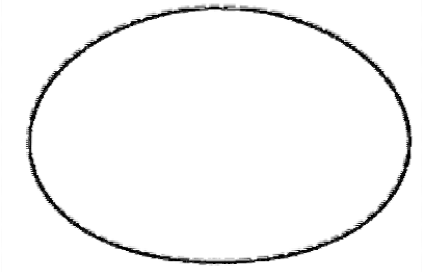

(c) log$M$(σ_0) = –3.9, d = 5.23 mm

Fig. 3 Comparisons of bubble shapes between at lower position (solid line) and at upper position (thick broken line)

Table 1 Fluid properties

log$M$(σ_0)	ρ_L [kg/m^3]	μ_L [mPa·s]	σ_0 [N/m]
–8.0	1116	4.4	0.069
–6.7	1154	9.3	0.068
–3.9	1205	46.7	0.067

*ρ_G = 1.2 kg/m^3 and $\mu_G = 1.8 \times 10^{-5}$ Pa·s

Table 2 Surface tension, σ_{eq}, [N/m] at adsorption-desorption equilibrium *

log$M(\sigma_0)$	C_T [mol/m^3]		C_O [mol/m^3]	
	0.10	0.20	2.39	3.25
−8.0	0.042 (−7.4)	0.036 (−7.2)	0.041 (−7.3)	0.038 (−7.2)
−6.7	0.044 (−6.1)	0.038 (−5.9)	0.044 (−6.1)	0.039 (−5.9)
−3.9	0.047 (−3.5)	0.043 (−3.3)	0.049 (−3.5)	0.046 (−3.4)

*values in parentheses represent log$M(\sigma_{eq})$

Table 3 Relevant dimensionless groups

Dimensionless group	Definition	Range
Morton number M	Eq. (2)	$10^{-7} < M < 10^{-3}$
Reynolds number Re	Eq. (12)	$3.6\times10^{-1} < Re < 1.7\times10^{2}$
Eötvös number Eo	Eq. (5)	$1.1\times10^{-1} < Eo < 5.9$
Weber number We	Eq. (6)	$5.0\times10^{-3} < We < 3.7$
Tadaki number Ta	Eq. (11)	$5.3\times10^{-2} < Ta < 3.6$

*the surface tension of a clean interface is used in evaluations of M, Eo, We and Ta in this table.

Examples of E and V_B of bubbles contaminated with Triton X-100 at log$M(\sigma_0)$ = −8.0 and −3.9 and C_T = 0.10 mol/m^3 are shown in Fig. 2, where C_T is the concentration of Triton X-100, σ_0 the surface tension of a clean interface, and M the Morton number defined by

$$M(\sigma_0) = \frac{\mu_L^4 \Delta\rho g}{\rho_L^2 \sigma_0^{\ 3}} \tag{2}$$

where g is the acceleration of gravity, μ the viscosity, ρ the density, $\Delta\rho$ the density difference $\rho_L - \rho_G$, and the subscripts L and G denote the liquid and gas phases, respectively. The z in the figure is the vertical distance measured from the nozzle tip. The V_B and E did not change in the observed region, and therefore, the bubbles were in their terminal conditions. The bubble terminal velocity is denoted by V_T in the following. All the bubbles were confirmed to be in their terminal conditions for $z \geq 200$ mm even in the highest Reynolds number case (log$M(\sigma_0)$ = −8.0). Bubble images were therefore taken at z = 350 mm. The bubble shapes at the lower position and at the upper position are the same as shown in Fig. 3, which also confirmed that the bubbles reached their terminal conditions. Side images of bubbles were also taken by using an additional high-speed video camera to check the axisymmetry of the bubbles. Small differences between d and E calculated from the front and side images, i.e. less than 0.84 % and

1.0 % for d and E, respectively, confirmed that the bubbles were axisymmetric and rose rectilinearly without shape oscillation.

Air and glycerol-water solutions contaminated with surfactant were used for the gas and liquid phases, respectively. Water purified by a Millipore system (Elix 3) and pure glycerol (Kishida-Kagaku) were used for the glycerol-water solutions. Triton X-100 (Wako Pure Chemical Industries, 168-11805) and 1-octanol (Wako Pure Chemical Industries, 156-00146) were used for surfactant. The experiments were carried out at room temperature and atmospheric pressure. The liquid density and viscosity were measured using a densimeter (Ando Keiki Co., Ltd., JIS B7525) and a viscometer (A&D, SV-10), respectively. The surface tension was measured using the pendant bubble method (Lin et al., 1990). The liquid temperature, which was measured using a thermometer (Netsuken, SN3000), was kept at 25 $\pm$ 0.5 ^{o}C throughout the experiments. The uncertainties in the density, viscosity and surface tension estimated at 95% confidence were 0.01, 1.3 and 2.0%, respectively. Glycerol concentrations were 80, 62 and 47 wt.%, for which log$M(\sigma_0)$ were −3.9, −6.7 and −8.0, respectively, as shown in Table 1. Table 2 shows the surface tensions, σ_{eq}, of the static interface in the adsorption-desorption equilibrium, where C_O is the concentration of 1-octanol. The C_T were lower than CMC. The E and V_T of clean bubbles were also measured. The ranges of the relevant dimensionless groups are summarised in Table 3.

3. Results and discussion

3.1 Bubble terminal velocity and aspect ratio

Figure 4 shows V_T of contaminated bubbles. The V_T increases with increasing d. The V_T data of clean bubbles are also shown in the figure. The data agree well with V_T calculated using the drag correlation proposed by Rastello et al. (2011). The V_T of contaminated bubbles are lower than those of clean bubbles. This velocity reduction is known as the Marangoni effect (Framkin and Levich, 1947; Levich, 1962; Takagi et al., 2003). The V_T in all the cases, even at different surfactant concentrations, are almost the same. Many studies have made clear that the drag coefficient of a fully-contaminated spherical bubble is equal to that of a solid sphere due to the immobility of the interface

caused by the Marangoni effect (Levich, 1962; Takagi et al., 2003; Nalajala and Kishore, 2014). The solid lines in Fig. 4 show terminal velocities V_T^S of solid spheres calculated using the following drag correlation (Schiller and Nauman, 1933):

$$C_D = \frac{24}{Re_S}[1 + 0.15 Re_S^{0.687}] \tag{3}$$

where Re_S is the particle Reynolds number defined by

$$Re_S = \frac{\rho_L V_T^S d}{\mu_L} \tag{4}$$

The V_T data agree well with V_T^S. Hence the bubbles were fully-contaminated from the point of view of V_T. The V_T at large d are slightly lower than V_T^S. This trend can be attributed to flattened shape of a bubble since a similar shape effect on V_T^S was also confirmed for ellipsoidal solid particles (Clift et al., 1978; Militzer et al., 1989). The drag coefficients of bubbles contaminated with surfactant were compared with Eq. (3) in Appendix A1.

Examples of shapes of clean and contaminated bubbles are shown in Fig. 5. The shape deformation of a contaminated bubble (Fig. 5 (c), E = 0.93) is slightly smaller than those of a clean bubble (Fig. 5 (a), E = 0.89). The difference in the shape between larger bubbles is more obvious as shown in Figs. 5 (d) and (b). The same trends can be seen in the other bubbles from (e) to (j).

The E of contaminated bubbles are plotted against d in Fig. 6. The E of clean bubbles are also shown in the figure. The E decreases with increasing d. It is clear that the presence of surfactant increases E in spite of the decrease in σ by surfactant. This increase in E might be attributed to the large reduction of V_T, in other words, the reduction of the dynamic pressure at the bubble nose, by surfactant as shown in Fig. 4. Comparing the E data of C_T = 0.1 mol/m^3 with those of C_T = 0.2 mol/m^3 shows that the increase in C_T, i.e. the decrease in σ, reduces E even in the fully-contaminated condition. The same trend is confirmed in the 1-octanol data. As shown in Figs. 5 (a) and (b), the clean bubbles have fore-aft symmetry, whereas the symmetry breaks in the contaminated bubbles. This might be due to a non-uniform interfacial distribution of

surfactant concentration, i.e. the surfactant concentration at the bubble interface increases from the bubble nose toward the tail due to advection (Cuenot et al., 1997).

In Fig. 7, E of contaminated bubbles are plotted against the Eötvös number defined by

$$Eo(\sigma) = \frac{\Delta\rho g d^2}{\sigma} \tag{5}$$

As shown in Fig. 7 (a), the E data are slightly scattered even at a constant M, which confirms that σ_0 is inappropriate to correlate E of contaminated bubbles. The scatter of the E data in Fig. 7 (b) is negligible, which implies that σ_{eq} can be used in correlating E instead of the actual surface tension at the interface of rising bubbles under the fully-contaminated condition. Therefore the dimensionless groups such as Eo and M will be calculated using σ_{eq} in the following.

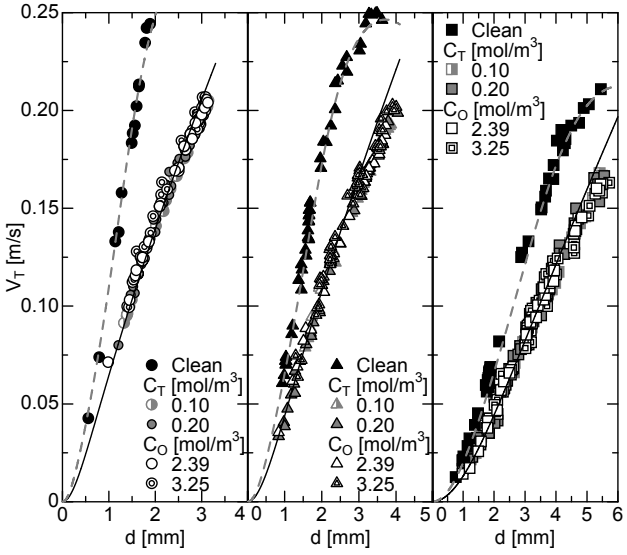

(a) log$M(\sigma_0)$ = –8.0 (b) –6.7 (c) –3.9

Fig. 4 Terminal velocity
(Solid lines: Eq. (3), Broken lines: V_T calculated using Rastello's drag correlation (Rastello et al., 2011) and Aoyama's E correlation (Aoyama et al., 2016) for clean bubble)

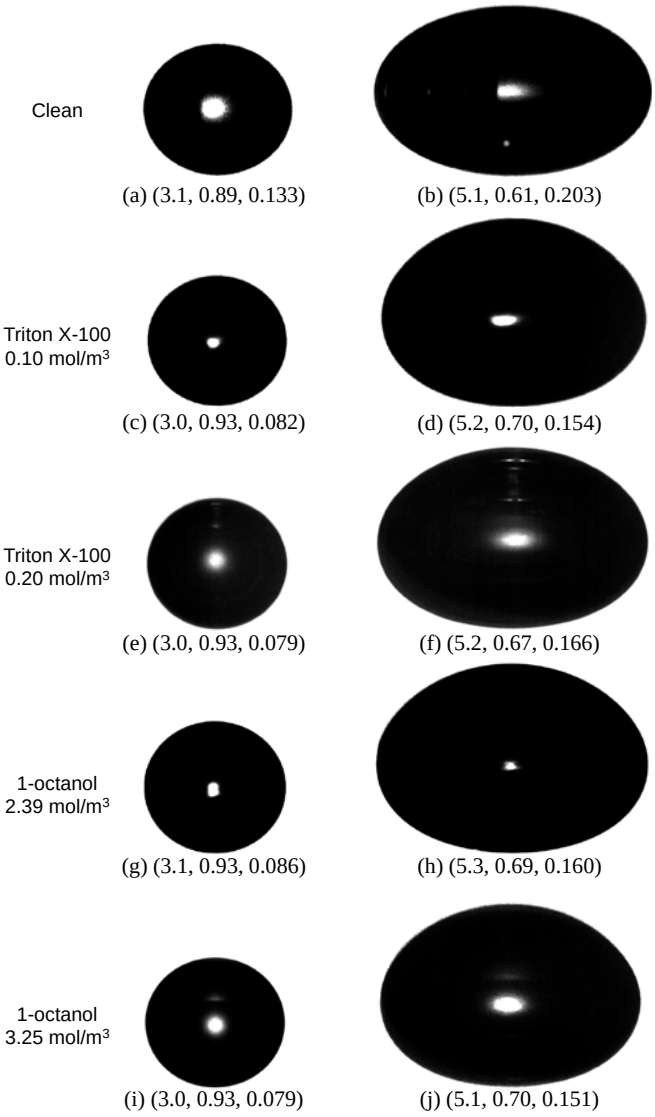

Fig. 5 Bubble shapes at $\log M(\sigma_0) = -3.9$
(values in parentheses represent (d [mm], E, V_T [m/s]))

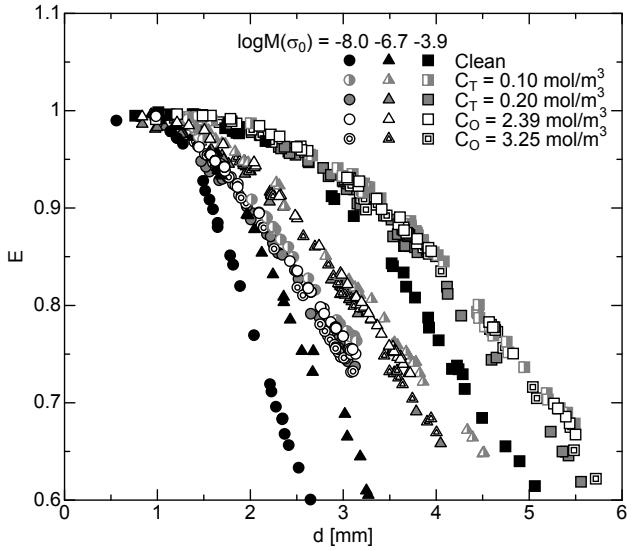

Fig. 6 Bubble aspect ratio

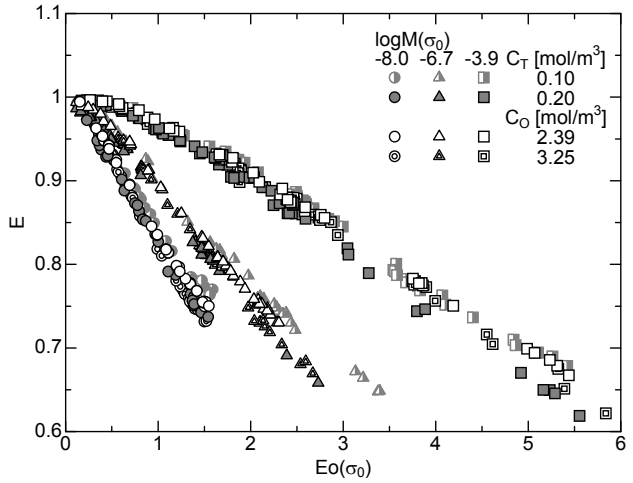

(a) E vs. $Eo(\sigma_0)$

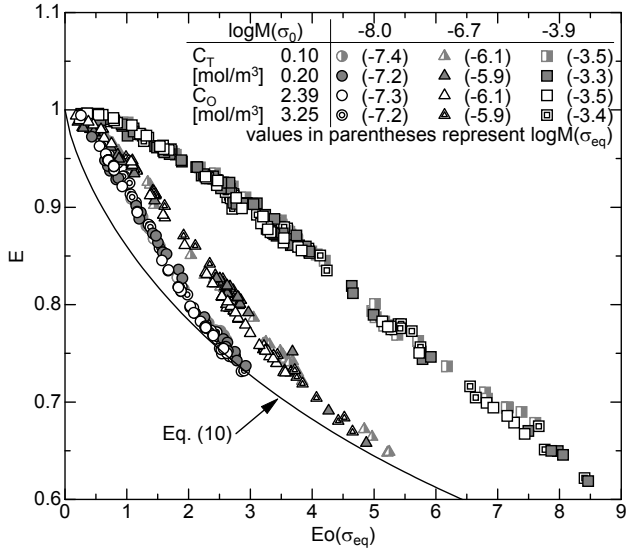

(b) E vs. $Eo(\sigma_{eq})$

Fig. 7 Dependence of E on surfactant concentration

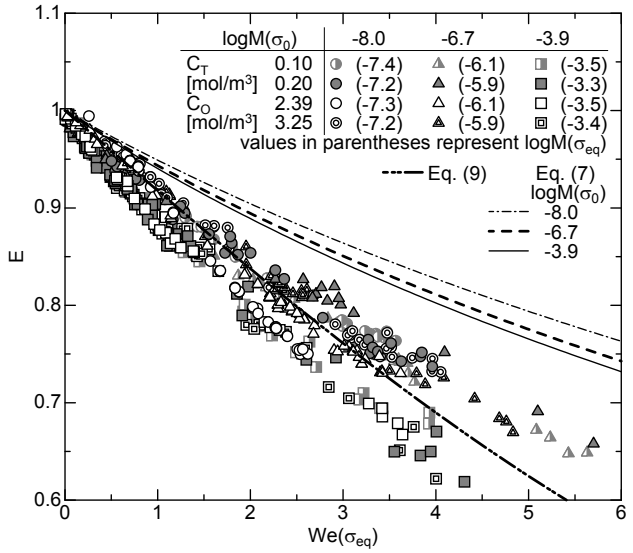

Fig. 8 Relation between E and $We(\sigma_{eq})$

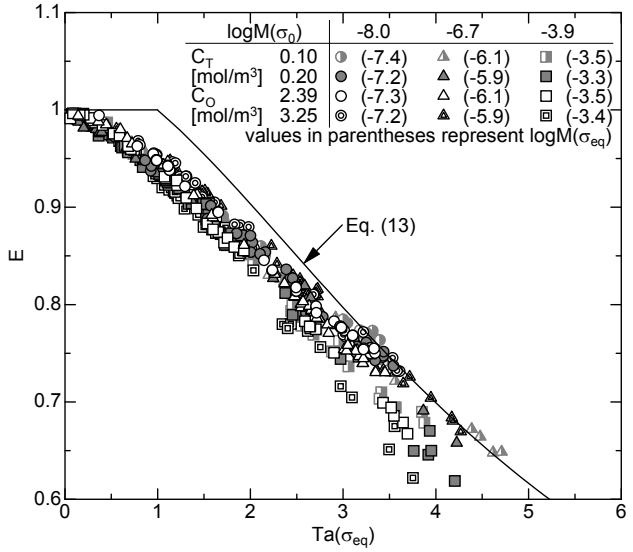

Fig. 9 Relation between E and $Ta(\sigma_{eq})$

3.2 Correlations of E for contaminated bubbles

The bubble aspect ratio has often been correlated (Moore, 1965; Wellek et al., 1966; Sugihara et al., 2007; Loth, 2008) in terms of the Weber number, *We*, defined by

$$We(\sigma) = \frac{\rho_L V_T^{\,2} d}{\sigma} \tag{6}$$

The E data are plotted against $We(\sigma_{eq})$ in Fig. 8. The E decreases with increasing *We*.

The data largely scatter, confirming that the E data cannot be correlated in terms of We only. Wellek et al. (1966) measured the aspect ratio of contaminated drops and proposed the following correlation:

$$E = \frac{1}{1 + 0.093 We^{0.98} \kappa^{0.07}} \tag{7}$$

where κ is the viscosity ratio defined by

$$\kappa = \frac{\mu_G}{\mu_L} \tag{8}$$

The correlation overestimates the bubble aspect ratios as shown in Fig. 8. Loth (2008) proposed the following E correlation:

$$E = 1 - 0.75 \tanh(0.11 We) \tag{9}$$

which gives better evaluations of E than the Wellek correlation as shown in Fig. 8. Wellek et al. (1966) also expressed E in terms of the Eötvös number Eo as

$$E = \frac{1}{1 + 0.163 Eo^{0.757}} \tag{10}$$

Tomiyama et al. (2002a) measured E of contaminated bubbles with zigzagging motion in an air-water system ($\log M = -11$) and reported that Eq. (10) agreed well with the measured data. However, in the case of contaminated bubbles with rectilinear motion, E depends not only on Eo but also on M, so that this correlation including only Eo is not applicable to the present data as shown in Fig. 7(b).

Tadaki and Maeda (1961) measured E of clean and contaminated bubbles in various Morton number systems and used the Tadaki number, Ta, to correlate E:

$$Ta = ReM^{0.23} \tag{11}$$

where *Re* is the bubble Reynolds number defined by

$$Re = \frac{\rho_L V_T d}{\mu_L} \tag{12}$$

Vakhrushev and Efremov (1970) proposed a correlation of E for contaminated bubbles in terms of *Ta*. Fan and Tsuchiya (1990) modified the Vakhrushev-Efremov correlation as follows:

$$E = \begin{cases} 1 & \text{for } Ta \le 1 \\ [0.81 + 0.206 \tanh\{2(0.8 - \log_{10} Ta)\}]^3 & \text{for } 1 \le Ta \le 39.8 \\ 0.24 & \text{for } Ta \ge 39.8 \end{cases} \tag{13}$$

Figure 9 shows E plotted against $Ta(\sigma_{eq})$. The Tadaki number can be expressed by the four relevant forces, i.e. the inertial F_i, the viscous F_μ, the buoyancy F_b and the surface tension forces F_σ, as $Ta = F_i^{0.54} F_b^{0.23} / F_\sigma^{0.69} F_\mu^{0.08}$, where

$$F_i = \rho_L V_T^{\,2} d^2 \tag{14}$$

$$F_b = \Delta\rho g d^3 \tag{15}$$

$$F_\mu = \mu_L V_T d \tag{16}$$

$$F_\sigma = \sigma d \tag{17}$$

It should be noted that $Re = F_i / F_\mu$ and $M = F_\mu^4 F_b / F_i^2 F_\sigma^3$. Equation (13) is compared with the E data in Fig. 9. Although *Ta* is much better than *We* and *Eo*, Eq. (13) overestimates the data. As shown in Fig. 10 (a), the following expression of E in terms of $Ta(\sigma_{eq})$ gives better evaluations of E:

$$E = \frac{1}{[1 + 0.00019 Ta(\sigma_{eq})^{1.34}]^{315}} \tag{18}$$

Figure 10 (b) shows comparisons between the data and E calculated using Eq. (18). Most of the data lie to within $\pm$5% errors.

The authors (Aoyama et al., 2016) proposed the following empirical correlation of E for clean bubbles:

$$E = \frac{1}{[1 + 0.016 Eo^{1.12} Re]^{0.388}} \tag{19}$$

The factor $Eo^{1.12}Re = (F_b/F_\sigma)^{1.12}(F_i/F_\mu)$ implies that the contributions of F_b, F_σ, F_i and F_μ to E are comparable with each other for clean bubbles. For contaminated bubbles, the coefficients should be modified since the balance of the relevant forces differs from that of a clean bubble. Let us make use of the same functional form, i.e.

$$E = \frac{1}{[1 + pEo^{\alpha} Re^{\beta}]^{q}} \tag{20}$$

where p, q, α and β are constants. Applying the least-square fitting to the experimental data yields

$$E = \frac{1}{[1 + 0.024 Eo(\sigma_{eq})^{1.17} Re^{0.44}]^{0.57}} \tag{21}$$

The constants, α and β, in Eq. (20) represent the contributions of Eo and Re to E, respectively. The α in the clean and contaminated cases take similar values, i.e. $\alpha \sim 1.1$. On the other hand, β in the contaminated system is about a half of that in the clean system. Therefore the effects of F_i and F_μ on E are weaker than those of F_b and F_σ in the fully-contaminated systems. The measured aspect ratios are plotted against $Eo(\sigma_{eq})^{1.17}Re^{0.44}$ in Fig. 11. The data are collapsed onto a single curve. E evaluated using Eq. (21) are to within $\pm$5% errors as shown in Figs. 11 (a) and (b). This correlation gives a better evaluation of E than Eq. (18), i.e. the root mean squared errors for Eqs. (18) and (21) are 0.019 and 0.011, respectively.

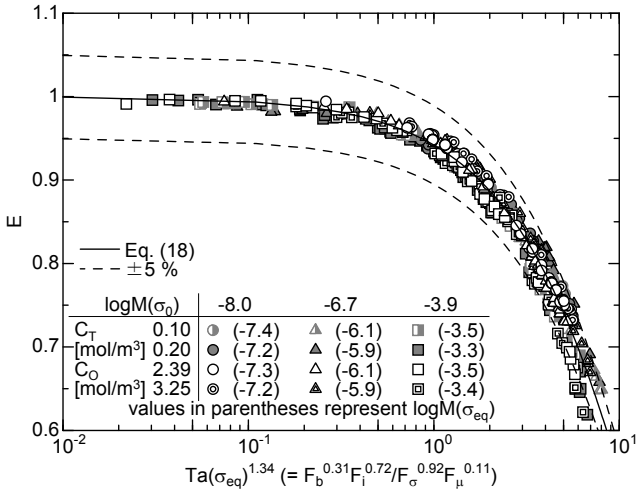

(a) E vs. $Ta(\sigma_{eq})^{1.34}$

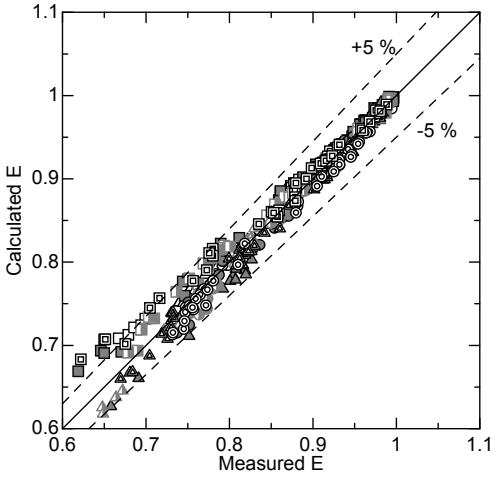

(b) Comparison between calculated and measured E

Fig. 10 Empirical correlation of E in terms of Ta

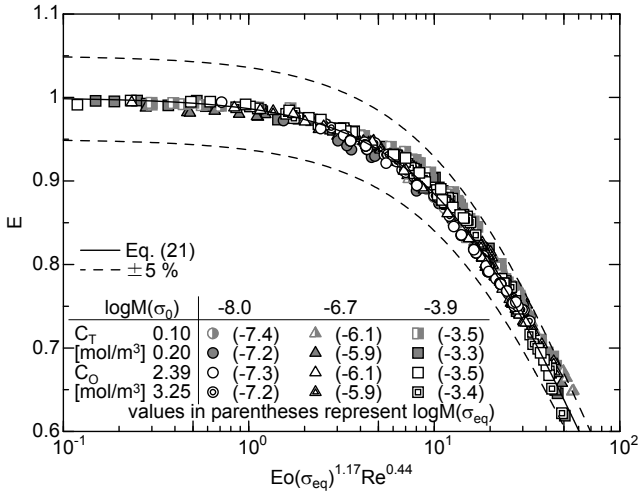

(a) E vs. $Eo(\sigma_{eq})^{1.17}Re^{0.44}$

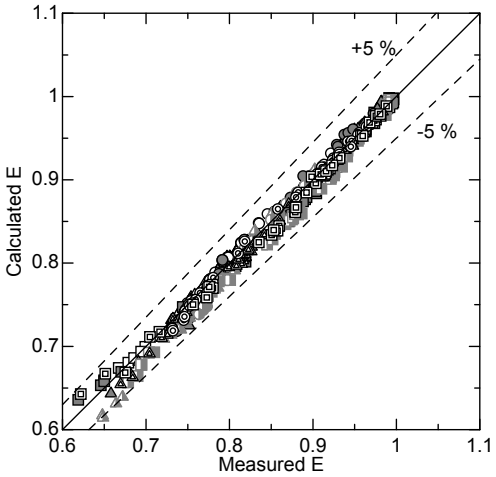

(b) Comparison between calculated and measured E

Fig. 11 E of contaminated bubbles correlated in terms of $Eo(\sigma_{eq})^{1.17}Re^{0.44}$

3.3 E in SDS and 1-decanol solutions

The empirical correlation of E for contaminated bubbles is applied to bubbles fully-contaminated with different surfactants in the following. Sodium dodecyl sulphate (SDS) (Serva, 20765) and 1-decanol (Wako Pure Chemical Industries, 048-24925) were used for surfactant. SDS and Triton X-100 form micelles at concentrations larger than CMC. SDS is anionic surfactant, whereas Triton X-100 is non-ionic surfactant. 1-decanol has a longer carbon chain length than 1-octanol. Table 4 shows σ_{eq}, where C_S and C_{DE} are the concentrations of SDS and 1-decanol, respectively. C_S = 5.0 mol/m^3 at

log$M(\sigma_0)$ = –8.0 and –6.7, whereas the higher concentration, i.e. C_S = 12.0 mol/m^3, was used at log$M(\sigma_0)$ = –3.9 to realize the fully-contaminated condition. The V_T data in these conditions agreed well with the data in Fig. 4, and therefore, bubbles contaminated with SDS and 1-decanol were confirmed to be fully-contaminated. Their C_D are shown in Appendix A1. Figure 12 shows comparisons between Eq. (21) and the E data for SDS and 1-decanol. The agreements are good. Hence the factor, $Eo(\sigma_{eq})^{1.17}Re^{0.44}$, is useful to correlate not only E of bubbles contaminated with Triton X-100 and 1-octanol but also those with SDS and 1-decanol. Even though Eq. (20) is fitted to all the data including, SDS and 1-decanol, the differences in the coefficients are small, i.e. (p, q, α, β) = (0.028, 0.44, 1.17, 0.47). Equation (21) is therefore applicable to all the surfactants examined.

Table 4 Surface tension, σ_{eq}, [N/m] at adsorption-desorption equilibrium†

log$M(\sigma_0)$	SDS*	1-decanol**
–8.0	0.038 (–7.2)	0.049 (–7.5)
–6.7	0.040 (–6.0)	0.049 (–6.3)
–3.9	0.040 (–3.2)	0.058 (–3.9)

*C_S = 5.0 mol/m^3 at log$M(\sigma_0)$ = –8.0 and –6.7, whereas 12.0 mol/m^3 at log$M(\sigma_0)$ = –3.9,
**C_{DE} = 0.16 mol/m^3,
†values in parentheses represent log$M(\sigma_{eq})$

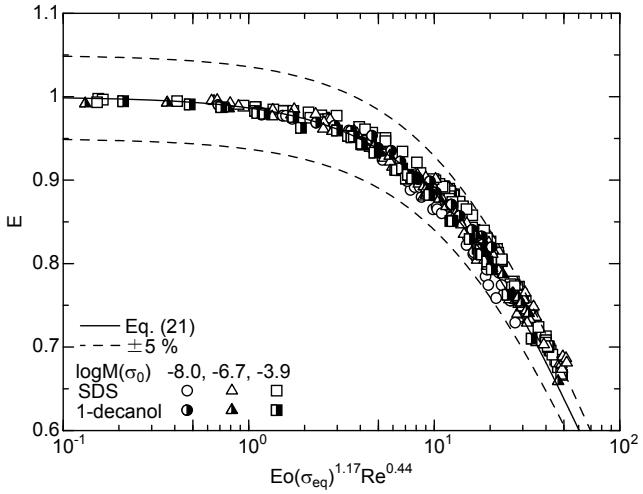

Fig. 12 Comparison between Eq. (21) and data of bubbles contaminated with SDS and 1-decanol

4. Conclusions

Shapes of single bubbles contaminated with Triton X-100 and 1-octanol rising through infinite stagnant liquids were measured by using a high-speed video camera for a wide range of fluid properties to investigate effects of surfactant on the bubble aspect ratio, E. The bubbles were fully-contaminated, i.e. their terminal velocities were independent of the surfactant concentration. The applicability of available correlations was examined through comparisons with the data. An empirical correlation of the aspect ratio was developed using the data and its applicability to bubbles in SDS and 1-decanol solutions were also examined. As a result, the following conclusions were obtained:

(1) Experimental databases of E of bubbles in fully-contaminated systems were obtained. Representative data of E are summarized in Appendix A2.
(2) Available E correlations for contaminated bubbles, i.e. the Fan-Tsuchiya and the Wellek correlations, are not applicable to the present data in the ranges of $3.6\times10^{-1} < Re < 1.7\times10^{2}$, $2.1\times10^{-1} < Eo < 8.5$ and $-8.0 \leq \log M \leq -3.9$.
(3) The E of fully-contaminated bubbles were well correlated in terms of a combination of the Eötvös number, Eo, and the bubble Reynolds number, Re, i.e. $Eo^{1.17}Re^{0.44}$, where Eo is evaluated using the surface tension at the adsorption-desorption equilibrium, σ_{eq}.
(4) The empirical correlation of E, Eq. (21), for fully-contaminated bubbles is applicable to bubbles contaminated with Triton X-100, SDS, 1-octanol and 1-decanol.

Acknowledgment

The authors would like to express their thanks to Mr. Toshihiko Takegawa for his assistance. This work was supported by JSPS KAKENHI Grant Number 15H03920.

Appendix

A1. Drag coefficients of bubbles in fully-contaminated systems

To check the degree of contamination of bubbles, the drag coefficients C_D of bubbles contaminated with surfactant were compared with those of solid spheres, Eq. (3). Figure A1 shows C_D at two surfactant concentrations for each surfactant, i.e. Triton X-100 and 1-octanol. The increase in the surfactant concentration does not affect C_D, and therefore, the bubbles are fully-contaminated at these concentrations. The C_D of bubbles contaminated with SDS and 1-decanol also agree with those with Triton X-100 and 1-octanol. In addition, the data agree well with Eq. (3).

A2. Aspect ratio data

Representative data of the aspect ratio, diameter, velocity, Eötvös number and Reynolds number of fully-contaminated bubbles are given in Tables A1, A2 and A3.

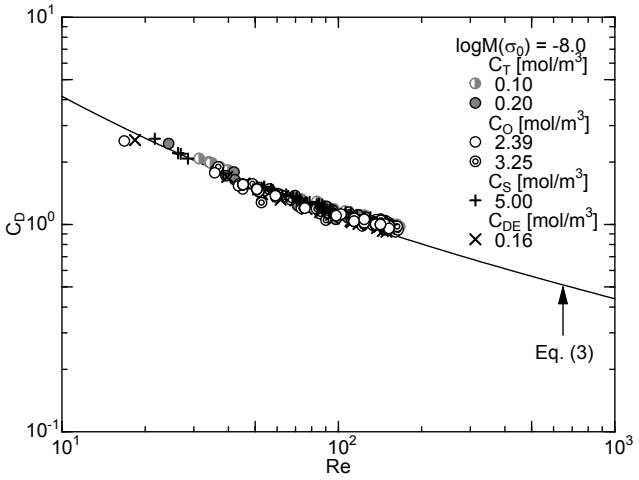

(a) log$M(\sigma_0)$ = –8.0

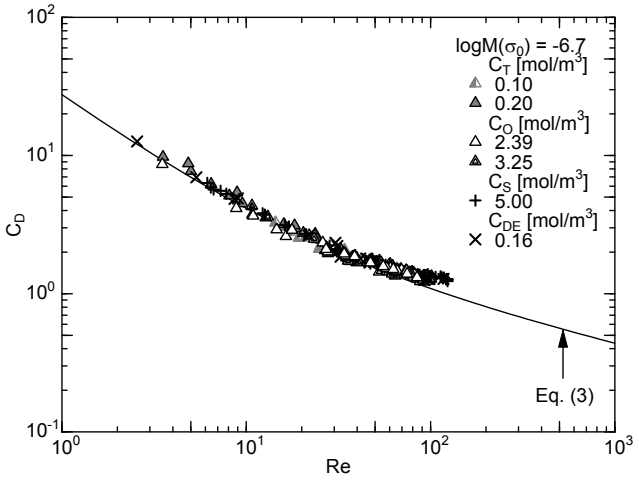

(b) log$M(\sigma_0)$ = –6.7

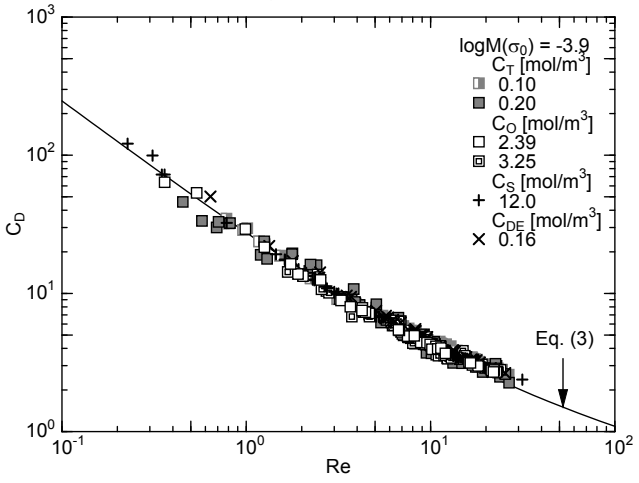

(c) log$M(\sigma_0)$ = –3.9

Fig. A1 Drag coefficients of contaminated bubbles

Table A1 Aspect ratio data ($\log M(\sigma_0) = -8.0$)

	E	d [mm]	V_T [m/s]	$Eo(\sigma_{eq})$	Re
Triton X-100	0.97	1.21	0.080	0.44	24.3
0.20 mol/m^3	0.93	1.70	0.121	0.86	51.9
σ_{eq} = 0.036 N/m	0.85	2.34	0.161	1.64	95.3
	0.75	3.03	0.203	2.75	155
1-octanol	0.97	1.40	0.100	0.59	35.9
3.25 mol/m^3	0.91	1.90	0.137	1.09	67.3
σ_{eq} = 0.038 N/m	0.86	2.26	0.160	1.53	92.8
	0.75	3.01	0.201	2.72	156
SDS	0.98	1.24	0.086	0.43	26.9
5.0 mol/m^3	0.94	1.75	0.122	0.85	53.9
σ_{eq} = 0.038 N/m	0.86	2.34	0.163	1.53	95.8
	0.76	2.97	0.196	2.45	146
1-decanol	0.99	1.04	0.073	0.24	18.4
0.16 mol/m^3	0.96	1.72	0.127	0.67	53.0
σ_{eq} = 0.049 N/m	0.90	2.34	0.169	1.23	96.1
	0.82	2.99	0.206	2.01	149

Table A2 Aspect ratio data ($\log M(\sigma_0) = -6.7$)

	E	d [mm]	V_T [m/s]	$Eo(\sigma_{eq})$	Re
Triton X-100	0.98	0.977	0.041	0.28	5.01
0.20 mol/m^3	0.95	1.77	0.092	0.93	20.4
σ_{eq} = 0.038 N/m	0.80	3.09	0.160	2.85	62.4
	0.66	4.05	0.199	4.87	101
1-octanol	0.98	1.45	0.072	0.61	13.1
3.25 mol/m^3	0.90	2.36	0.135	1.61	39.8
σ_{eq} = 0.039 N/m	0.80	3.11	0.160	2.81	62.2
	0.67	4.00	0.202	4.65	101
SDS	1.00	1.11	0.051	0.35	6.64
5.0 mol/m^3	0.94	1.97	0.101	1.10	23.5
σ_{eq} = 0.040 N/m	0.82	3.16	0.165	2.84	61.4
	0.69	4.18	0.202	4.96	99.5
1-decanol	0.99	0.989	0.043	0.22	5.36
0.16 mol/m^3	0.96	1.83	0.095	0.76	21.8
σ_{eq} = 0.049 N/m	0.83	3.14	0.164	2.26	64.8
	0.66	4.40	0.212	4.44	117

Table A3 Aspect ratio data ($\log M(\sigma_0) = -3.9$)

	E	d [mm]	V_T [m/s]	$Eo(\sigma_{eq})$	Re
Triton X-100	0.99	1.19	0.022	0.39	0.71
0.20 mol/m^3	0.95	2.63	0.075	1.89	5.39
σ_{eq} = 0.043 N/m	0.82	4.12	0.131	4.64	14.8
	0.65	5.42	0.159	8.06	23.7
1-octanol	0.99	1.67	0.039	0.72	1.68
3.25 mol/m^3	0.96	2.57	0.070	1.71	4.67
σ_{eq} = 0.046 N/m	0.84	4.05	0.124	4.24	13.0
	0.62	5.72	0.163	8.40	24.0
SDS	0.99	1.00	0.013	0.30	0.35
12.0 mol/m^3	0.96	2.52	0.065	1.88	4.21
σ_{eq} = 0.040 N/m	0.83	4.06	0.118	4.86	12.4
	0.67	5.40	0.161	8.62	22.4
1-decanol	0.99	1.54	0.030	0.48	1.33
0.16 mol/m^3	0.96	2.62	0.068	1.39	5.07
σ_{eq} = 0.058 N/m	0.85	4.02	0.118	3.27	13.5
	0.71	5.43	0.164	5.96	25.4

References

Aoki, J., Hayashi, K., Hosokawa, S., Tomiyama, A., Effects of surfactants of mass transfer from single carbon dioxide bubbles in vertical pipes, *Chem. Eng. Tech.*, 38, pp. 1955-1964, 2015.

Aoyama, S., Hayashi, K., Hosokawa, S., Tomiyama, A., Shapes of ellipsoidal bubbles in infinite stagnant liquids, *Int. J. Multiphase Flow*, 79, pp. 23-30, 2016.

Bel Fdhila, R., Duineveld, P.C., The effect of surfactant on the rise of a spherical bubble at high Reynolds and Peclet numbers, *Physics of Fluids*, 8, pp. 310-321, 1996.

Clift, R., Grace, J.R., Weber, M.E., *Bubbles, drops, and particles*, Academic Press, 1978.

Cuenot, B., Magnaudet, J., Spennato, B., The effects of slightly soluble surfactants on the flow around a spherical bubble, *J. Fluid Mech.*, 339, pp. 25-53, 1997.

Fan, L.S., Tsuchiya, K., *Bubble wake dynamics in liquids and liquid-solid suspensions*, Butterworth-Heinemann, 1990.

Frumkin, A.N., Levich, V.G., The Motion of solid and liquid metal particles in electrolyte solutions. I: The motion in electric field, *Zh. Fiz. Khim*, 19, pp. 573-600, 1945.

Fukuta, M., Takagi, S., Matsumoto, Y., Numerical study on the shear-induced lift force acting on a spherical bubble in aqueous surfactant solutions, *Physics of Fluids*, *20*, 2008.

Lamb, H., *Hydrodynamics*, 6th Edition, Cambridge Univ. Press, 1932.

Legendre, D., Zenit, R., Velez-Cordero, J.R., On the deformation of gas bubbles in liquids, *Physics of Fluids*, 24, 043303, 2012.

Levich, V.G., *Physicochemical hydrodynamics*, Prentie-Hall, 1962.

Lin, S.Y., McKeigue, K., Maldarelli, C., Diffusion-controlled surfactant adsorption studied by pendant drop digitization, *AIChE J.*, 36, pp. 1785-1795, 1990.

Liu, L., Yan, H., Zhao, G., Experimental studies on the shape and motion of air bubbles in viscous liquids, *Experimental Thermal and Fluid Science*, 62, pp. 109-121, 2015.

Lochiel, A.C., Calderbank, P.H., Mass transfer in the continuous phase around axisymmetric bodies of revolution, *Chem. Eng. Sci.*, 19, pp. 471-484, 1964.

Loth, E., Quasi-steady shape and drag of deformable bubbles and drops, *Int. J. Multiphase Flow*, 34, pp. 523-546, 2008.

Moore, D.W., The velocity of rise of distorted gas bubbles in a liquid of small viscosity, *J. Fluid Mech.*, 23, pp. 749-766, 1965.

Militzer, J., Kan, J.M., Hamdullahpur, F., Amyotte, P.R., Al Taweel, A.M., Drag coefficient for axisymmetric flow around individual spheroidal particles, *Powder technology*, 57, pp. 193-195, 1989.

Myint, W., Hosokawa, S., Tomiyama, A., Shape of single drops rising through stagnant liquids, *J. Fluid Science and Technology*, 2, pp. 184-195, 2007.

Nalajala, V.S., Kishore, N., Drag of contaminated bubbles in power-law fluids, *Colloids and Surfaces A: Physicochemical. Eng. Aspects*, 443, pp. 240-248, 2014.

Rastello, M., Marié, J., Lance, M., Drag and lift forces on clean spherical and ellipsoidal bubbles in a solid-body rotating flow, *J. Fluid Mech.*, 682, pp. 434-459, 2011.

Raymond, F., Rosant, J.M., A numerical and experimental study of the terminal velocity and shape of bubbles in viscous liquids, *Chem. Eng. Sci.*, 55, pp. 943-955, 2000.

Schiller, V.L., Nauman, A.Z., Über die grundlegenden Berechnungen bei der Schwerkraftaufbereitung, *Zeitschridt des Vereines Deutscher Ingenieure*, 77, pp. 318-320, 1933.

Sugihara, K., Sanada, T., Shirota, M., Watanabe, M., Behavior of single rising bubbles in superpurified water, *Soc. Chem. Eng. Japan*, 33, pp. 402-408, 2007, in Japanese.

Tadaki, T., Maeda, S., On the shape and velocity of single air bubbles rising in various liquids, *Soc. Chem. Eng. Japan*, 25, pp. 254-264, 1961, in Japanese.

Takagi, S., Ogasawara, T., Fukuta, M., Matsumoto, Y., Surfactant effect on the bubble motions and bubbly flow structures in a vertical channel, *Fluid dynamics research*, 41, 2009.

Takagi, S., Uda, T., Watanabe, Y., Matsumoto, Y., Behavior of a rising bubble in water with surfactant dissolution (1st report, steady behavior), *Japan Soc. Mech. Eng. Series B*, 69, pp. 2192-2199, 2003, in Japanese.

Tomiyama, A., Kataoka, I., Žun, I., Sakaguchi, T., Drag coefficients of single bubbles under normal and micro gravity conditions, *JSME International Journal Series B Fluids and Thermal Engineering*, 41, pp. 472-479, 1998.

Tomiyama, A., Celata, G.P. Hosokawa, S., Yoshida, S., Terminal velocity of single bubbles in surface tension force dominant regime, *Int. J. Multiphase Flow*, 28, pp. 1497-1519, 2002a.

Tomiyama, A., Tamai, H., Žun, I., Hosokawa, S., Transverse migration of single bubbles in simple shear flows, *Chem. Eng. Sci.*, 57, pp. 1849-1858, 2002b.

Tomiyama, A., Drag, lift and virtual mass forces acting on a single bubble, *International Symposium on Two-Phase Flow Modelling and Experimentation*, 2004.

Vakhrushev, I.A, Efremov, G.I., Interpolation formula for computing the velocities of single gas bubbles in liquids, *Chem. Technol. Fuels Oils (USSR)*, 6, pp. 376-379, 1970.

Wellek, R.M., Agrawal, A.K., Skelland, A.H.P., Shape of liquid drops moving in liquid media, *AIChE J.*, 12, pp. 854-862, 1966.